12th International Symposium on Turbulence and Shear Flow Phenomena (TSFP12)
Osaka, Japan (Online), July 19-22, 2022

LARGE-SCALE CLUSTERING OF INERTIAL PARTICLES IN HOMOGENEOUS ISOTROPIC TURBULENCE

Keigo Matsuda
Japan Agency for Marine-Earth Science and Technology (JAMSTEC),
Yokohama, Japan
k.matsuda@jamstec.go.jp

Katsunori Yoshimatsu
Institute of Materials and Systems for Sustainability, Nagoya University
Nagoya, Japan
yoshimatsu@nagoya-u.jp

Kai Schneider
Institut de Mathématiques de Marseille (I2M)
Aix-Marseille Université, CNRS,
Marseille, France
kai.schneider@univ-amu.fr

ABSTRACT

The nonlinear dynamics of inertial particles in high Reynolds number turbulence, and in particular clustering and void formation, are important fundamental processes, for instance, for droplets in atmospheric clouds and rain formation. Here we analyze particle data from three-dimensional direct numerical simulations of particle-laden homogeneous isotropic turbulence at high Reynolds number, up to $Re_\lambda = 678$ and with up to 3.2×10^9 particles, computed at resolution 4096^3. We show that the particle density spectrum of the analyzed data has a bump at large scales for sufficiently high Reynolds number, in addition to the near-dissipation scale bump observed so far. The large-scale bump is attributed to large-scale clustering of inertial particles. We find that this behavior is generic and independent of the forcing scheme used to maintain a statistically stationary flow.

INTRODUCTION

Inertial particles suspended in high Reynolds number turbulence are ubiquitous in geophysical or industrial flows, such as cloud droplets in atmospheric turbulence, dust particles in protoplanetary disks, and fuel droplets in spray combustion. Inertial particles show nonuniform distribution, i.e., clustering, in turbulence due to the centrifugal effect because particles are swept out from turbulent vortices and concentrate in low vorticity regions (Maxey, 1987; Squires & Eaton, 1991). In atmospheric flows, turbulent clustering of cloud droplets can increase collision and coalescence frequency in raindrop formation process (Onishi & Vassilicos, 2014; Ireland *et al.*, 2016). The clustering can also affect the cloud radar reflectivity factor (Matsuda *et al.*, 2014; Matsuda & Onishi, 2019). Thus, for improving cloud microphysics models, it is important to understand the clustering behavior in high Reynolds number flow.

Even though the Reynolds-number dependence of inertial particle clustering has been studied extensively, the clustering behavior in high Reynolds number turbulence in atmospheric clouds ($Re_\lambda \sim 10^3$–10^5, where Re_λ is the Taylor microscale Reynolds number) is not fully understood. Large-scale flows could affect the particle clustering at such high Reynolds number. Matsuda *et al.* (2014) computed the particle number density spectrum, using direct numerical simulation (DNS) of particle-laden homogeneous isotropic turbulence. They observed a bump near the dissipation scale. Moreover they showed that the number density spectrum is intensified at large scales, i.e. at small wavenumbers, as the Reynolds number increases. This observation can arise a question whether large-scale clustering does occur or not. In this work, we aim to clarify the Reynolds-number dependence of the number density spectrum and, particularly, the large-scale clustering, using three-dimensional DNS of particle-laden homogeneous isotropic turbulence at high Reynolds number.

In the following, we first briefly describe the governing equations and the DNS approach. Numerical results showing spectra of turbulent kinetic energy and particle number density are discussed. Finally, some conclusions are given, and future work is motivated.

DIRECT NUMERICAL SIMULATION

A statistically homogeneous velocity field $\boldsymbol{u}(\boldsymbol{x},t)$ of an incompressible fluid was obtained by the Navier–Stokes equation:

$$\frac{\partial \boldsymbol{u}}{\partial t} + (\boldsymbol{u}\cdot\nabla)\boldsymbol{u} = -\frac{1}{\rho}\nabla p + \nu\nabla^2\boldsymbol{u} + \boldsymbol{f}, \tag{1}$$

$$\nabla\cdot\boldsymbol{u} = 0, \tag{2}$$

where $\boldsymbol{f}(\boldsymbol{x},t)$ is an external solenoidal forcing, $p(\boldsymbol{x},t)$ is the pressure, ν is the constant kinematic viscosity, and ρ is the constant fluid density.

The particles were treated as point particles and tracked by the Lagrangian method. We assumed that the particle size is sufficiently smaller than the Kolmogorov scale η and the particle density ρ_p is sufficiently larger than the fluid density ρ. Then, Lagrangian motion of inertial heavy particles was

tracked by integrating the following equations:

$$\frac{d\boldsymbol{x}_p}{dt} = \boldsymbol{v}, \tag{3}$$

$$\frac{d\boldsymbol{v}}{dt} = -\frac{\boldsymbol{v}-\boldsymbol{u}(\boldsymbol{x}_p)}{\tau_p}, \tag{4}$$

where $\boldsymbol{x}_p$ and $\boldsymbol{v}$ are the position and velocity of a Lagrangian particle, respectively, and τ_p is the relaxation time of particle motion.

Equations (1) and (2) were solved in a cubic computational domain with periodic boundary conditions. The domain has side length of 2π and is discretized by Cartesian staggered grids. The fourth-order central-difference schemes were used for the advection and viscous terms (Morinishi *et al.*, 1998) and the second-order Runge–Kutta scheme was used for time integration. The velocity and pressure were coupled by the HSMAC method (Hirt & Cook, 1972).

To clarify the influence of the external forcing for turbulence on the large-scale clustering, we applied two types of forcing schemes: large-scale linear forcing (LF) and large-scale random forcing (RF). The large-scale linear forcing is applied to the large-scale flow where the wavenumber k is smaller than 2.5. The forcing $\boldsymbol{f}$ is proportional to the large-scale velocity $\boldsymbol{u}_{k<2.5}$ (Onishi *et al.*, 2011), where $\boldsymbol{u}_{k<2.5}$ is the low-pass filtered velocity field, retaining the energy of Fourier modes only for $k < 2.5$. The large-scale random forcing is in accordance with the velocity forcing proposed by Yoshida & Arimitsu (2007). In this case, the forcing $\boldsymbol{f}$ is similarly applied for $k < 2.5$ but changes randomly, having a correlation time of T_f. We set $T_f = 1$ to be close to the large-eddy turnover time.

The important parameters in this study are the Taylor-microscale Reynolds number $Re_\lambda \equiv u'\lambda/\nu$ and the Stokes number $St \equiv \tau_p/\tau_\eta$, where u' is the root-mean-square velocity fluctuation, λ is the Taylor microscale, and τ_η is the Kolmogorov time. The DNS with the linear forcing was performed for $Re_\lambda = 204$, 328, and 531, using 512^3, 1024^3, and 2048^3 grid points, respectively. The DNS with the random forcing was carried out for $Re_\lambda = 155$, 251, 402, and 678, using 512^3, 1024^3, 2048^3, and 4096^3 grid points, respectively. In all simulations, the Stokes number was set to 1.0. The number of particles is in maximum 3.2×10^9. The initial particle distribution is random and homogeneous. The flow velocity and particle distribution data were sampled after the time integration of $10T_f$, and 10 snapshots of three-dimensional data were saved at interval of T_f. The statistical results are obtained by averaging over 10 snapshots.

RESULTS AND DISCUSSIONS

Figure 1 shows time-averaged turbulent kinetic energy spectra for different Reynolds numbers, for two different forcing mechanisms, either large-scale linear forcing (LF) or random forcing (RF). In the large Reynolds number case, $Re_\lambda = 678$, a $k^{-5/3}$ power law behavior can be observed for about one decade in the normalized wavenumber $k\eta$.

We also calculate the particle number density spectrum. It should be noted that the number density spectrum is typically contaminated by Poisson noise. In this work, the Poisson noise is removed from the spectrum by applying an analytical Fourier transform directly to Lagrangian particle data (Matsuda *et al.*, 2014; Matsuda & Onishi, 2019). Due to high computational cost of the direct evaluation of Fourier transform, the spectrum values are calculated for 19 selected wavenumbers at $k = 1$, 2, 3, 4, 6, 8, 12, 16, 24, 32, 48, 64, 96, 128, 192, 256, 384, 512, and 768. Figure 2 shows the time-averaged number density spectra for $St = 1.0$. The number density spectra for the linear forcing illustrate the influence of Re_λ at small wavenumbers ($k\eta \lesssim 0.03$), as reported by Matsuda *et al.* (2014). The spectra for the random forcing also show the similar Re_λ dependence; i.e., for both forcing schemes, the particle density spectra exhibit two well pronounced bumps when Re_λ is larger than 300. The bump at larger scale is attributed to large-scale clustering of inertial particles. Therefore, the large-scale clustering is generic and independent of the two forcing

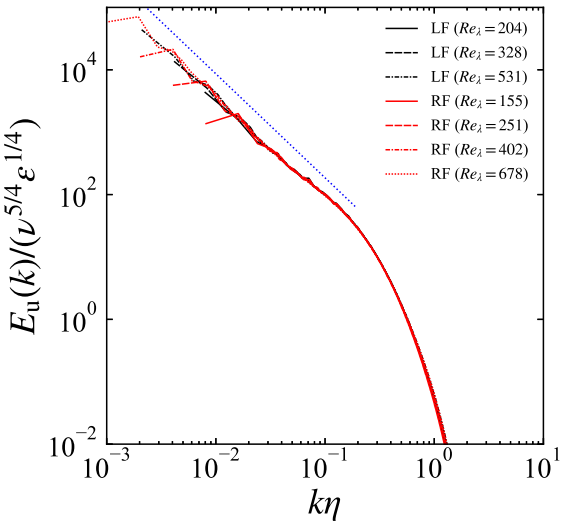

Figure 1. Turbulent kinetic energy spectra for different Reynolds numbers using the large-scale linear forcing (LF) and random forcing (RF) schemes as a function of $k\eta$. The dotted line corresponds to $k^{-5/3}$.

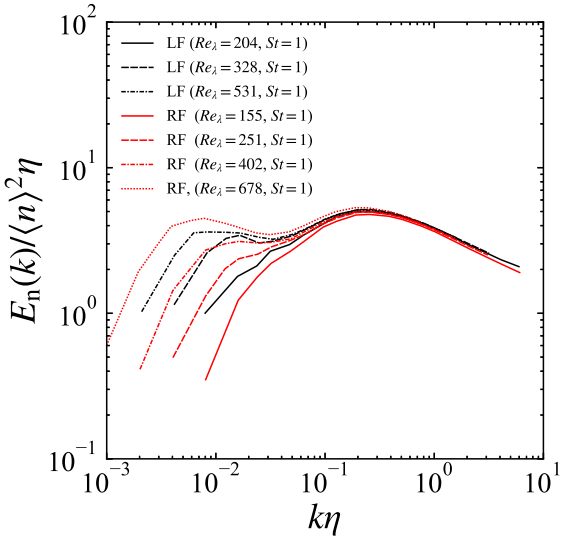

Figure 2. Particle number density spectra for $St = 1$ at different Reynolds numbers using the large-scale linear forcing (LF) and random forcing (RF) schemes as a function of $k\eta$.

schemes used to maintain statistically stationary flows.

Recently, in Matsuda *et al.* (2021), we performed wavelet analyses of inertial particle distribution, and a signature of void-pronounced structure was observed at $k\eta \lesssim 0.02$ for $Re_\lambda > 300$. Thus, we conjecture that the large-scale clustering could be related to such large-scale voids. For illustration, a snapshot of the spatial distribution of particles in a slice of thickness 4η is presented in figure 3 for $Re_\lambda = 678$ using the RF scheme. The inhomogeneous particle distribution shows large pronounced void regions and accumulated clusters. To clarify the mechanism of the large-scale clustering, assessing the convergence and divergence of particles is crucial. For instance, Oujia *et al.* (2020) introduced a finite time measure to quantify the convergence and divergence of the particle velocity using Voronoi tessellation. They showed that divergence is the most prominent in cluster regions and less pronounced in void regions. It was also found that for larger volumes, negative divergence values are observed which represent cluster formation (i.e. particle convergence). For small volumes, positive divergence values are found which correspond to cluster destruction/void formation (i.e. particle divergence). Applying this technique to high Reynolds number particle-laden flows will yield deeper insight into the dynamics of large-scale clustering.

CONCLUDING REMARKS

Reynolds-number dependence of inertial heavy particle clustering has been investigated by using three-dimensional DNS of particle-laden homogeneous isotropic turbulence. The DNS was performed for several Reynolds numbers up to $Re_\lambda = 678$ and two cases of large-scale forcing schemes (the linear and random forcing schemes) to maintain statistically stationary turbulence. The number of particles was in maximum 3.2×10^9. The Stokes number was fixed to 1.0. The analyzed data show that for $Re_\lambda > 300$ the particle density spectra exhibit two well pronounced bumps. The bump at larger scale is attributed to large-scale clustering of inertial particles. This behavior is generic and independent of the forcing scheme. Further investigation of the large-scale clustering mechanism will be performed, the influence of the Stokes number will be assessed and elaborated analyses of the spectral bumps will be published in forthcoming work.

ACKNOWLEDGEMENTS

K.M. acknowledges financial support from Grant-in-Aid for Scientific Research (C) No. JP20K04298 from the Japan Society for the Promotion of Science (JSPS). K.S. acknowledges funding from the Agence Nationale de la Recherche (ANR), grant ANR-20-CE46-0010-01 and the French Research Federation for Fusion Studies within the framework of the European Fusion Development Agreement (EFDA). He also acknowledges kind hospitality during his visit at JAMSTEC and financial support. The present DNS was performed on the Earth Simulator supercomputer system of JAMSTEC.

REFERENCES

Hirt, C. W. & Cook, J. L. 1972 Calculating three-dimensional flow around structures and over rough terrain. *J. Comput. Phys.* **10**, 324–340.

Ireland, P. J., Bragg, A. D. & Collins, L. R. 2016 The effect of Reynolds number on inertial particle dynamics in isotropic turbulence. Part 2. simulations with gravitational effects. *J. Fluid Mech.* **796**, 617–658.

Matsuda, K. & Onishi, R. 2019 Turbulent enhancement of radar reflectivity factor for polydisperse cloud droplets. *Atmos. Chem. Phys.* **19**, 1785–1799.

Matsuda, K., Onishi, R., Hirahara, M., Kurose, R., Takahashi, K. & Komori, S. 2014 Influence of microscale turbulent droplet clustering on radar cloud observations. *J. Atmos. Sci.* **71**, 3569–3582.

Matsuda, K., Schneider, K. & Yoshimatsu, K. 2021 Scale-dependent statistics of inertial particle distribution in high Reynolds number turbulence. *Phys. Rev. Fluids* **6**, 064304.

Maxey, M. R. 1987 The gravitational settling of aerosol particles in homogeneous turbulence and random flow fields. *J. Fluid Mech.* **174**, 441–465.

Morinishi, Y., Lund, T. S., Vasilyev, O. V. & Moin, P. 1998 Fully conservative higher order finite difference schemes for incompressible flow. *J. Comput. Phys.* **143**, 90–124.

Onishi, R., Baba, Y. & Takahashi, K. 2011 Large-scale forcing with less communication in finite-difference simulations of steady isotropic turbulence. *J. Comput. Phys.* **230**, 4088–4099.

Onishi, R. & Vassilicos, J. C. 2014 Collision statistics of inertial particles in two-dimensional homogeneous isotropic turbulence with an inverse cascade. *J. Fluid Mech.* **745**, 279–299.

Oujia, T., Matsuda, K. & Schneider, K. 2020 Divergence and convergence of inertial particles in high Reynolds number turbulence. *J. Fluid Mech.* **905**, A14.

Squires, K. D. & Eaton, J. K. 1991 Measurements of particle dispersion obtained from direct numerical simulations of isotropic turbulence. *J. Fluid Mech.* **226**, 1–35.

Yoshida, K. & Arimitsu, T. 2007 Inertial-subrange structures of isotropic incompressible magnetohydrodynamic turbulence in the lagrangian renormalized approximation. *Phys. Fluids* **19**, 045106.

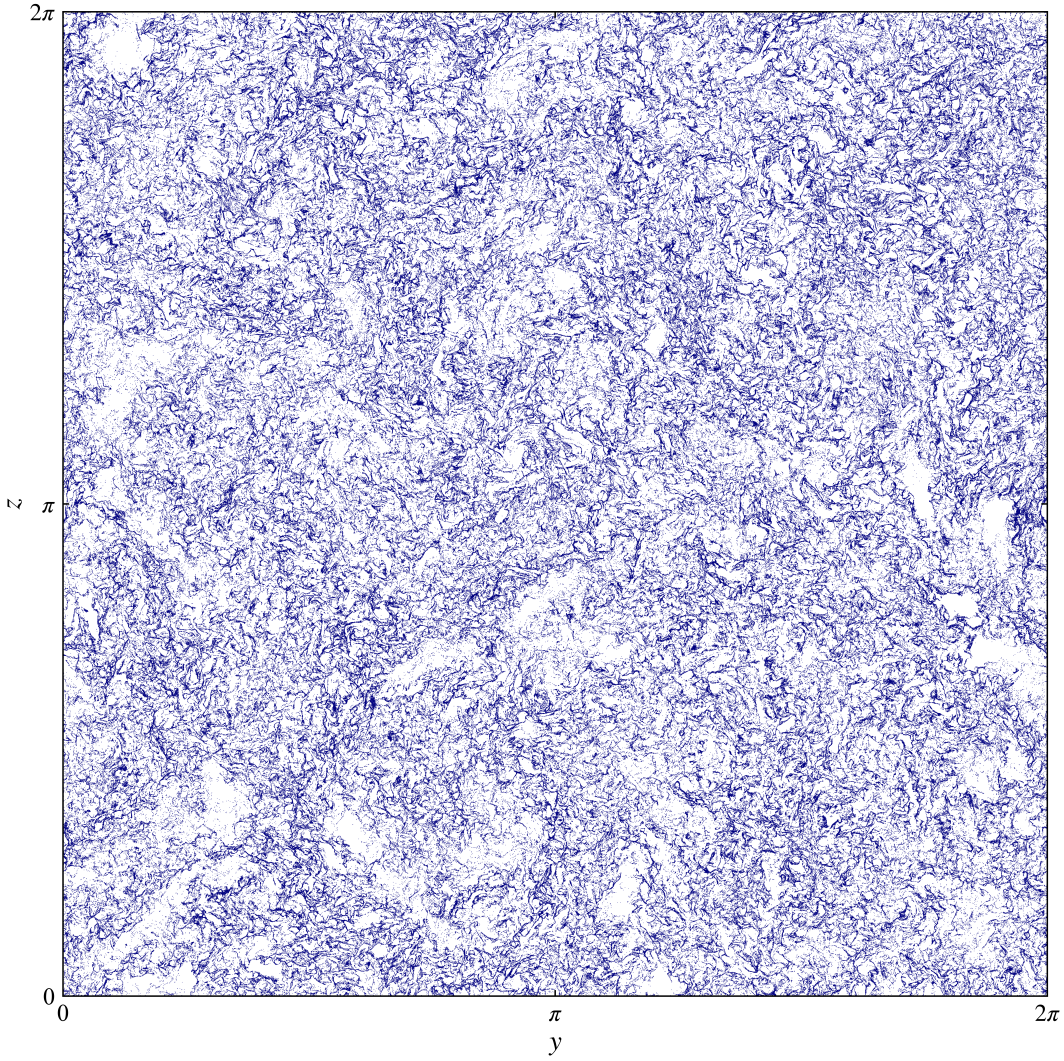

Figure 3. Spatial distribution of inertial particles for $Re_\lambda = 678$ using the RF scheme in a slice at $0 < x < 4\eta$.